AGC Regulator Design for Wind Farms

Esha Gupta, Akash Saxena
Department of Electrical Engineering
Swami Keshvanand Institute of Technology Management & Gramothan, Jaipur,
Email- esha.gupta@outlook.com, aakash.saxena@hotmail.com
Received 10 August 2015, received in revised form 12 September 2015, accepted 15 September 2015

Abstract: **The Automatic Generation Control is a mechanism to ensure the real power balance between generation and load. AGC plays an important role to keep the system frequency and tie line loadings in a nominal range. Increasing demand in wind generation shows an avenue to install wind power plants in the grid. The assessment of their impact on the frequency droop characteristics is the topic of interest. This paper investigated the effect of different wind penetration on two area thermal interconnected system. The closed loop eigenvalue analysis is carried out for different wind penetration levels to examine the system stability. The paper analyzed the working of the Doubly Fed Induction Generator (DFIG) as a supporter to the frequency of the grid and without its support. The gains of PI controller are optimized through newly introduced Grey Wolf Optimizer (GWO) technique. From the investigations carried out, it is found that with the dynamic participation of DFIG as a supporter of frequency of the grid improves the frequency response of the system.**

Keywords— **Automatic Generation Control (AGC); Integral Time multiplied Absolute Error (ITAE); Grey Wolf Optimizer(GWO); Doubly Fed Induction Generator(DFIG).**

1. INTRODUCTION

Now days, as the power demands are increasing, renewable energy power generating plants are explored. Integration of wind energy with the conventional thermal and hydro plants is going through a very rapid development of escalating load demands. The penetration of wind has greater impact on the power system dynamics. Power system dynamics is the study of the system behavior under perturbations and disturbances [1]. With wind integrated system the presence of variable speed generators and asynchronous generators effect system stability and dynamics in a prominent way [2]. To examine the effect of wind penetrations on small signal stability is primary motivation of this work. In large wind penetrated network, the number of synchronous units reduces which falls system inertia as rotating mass is less seen by the grid. The robustness of such system reduces for small load perturbations. Many researchers concentrate their work on this issue [3]. In these the control capability of DFIG wind turbine is explored for not only to increase the system inertia but also for frequency support to the grid. By application of these control methodologies penetration level of wind can be enhanced.

Recent approaches on the investigations of the inertia effect of DFIG summarized that introduction of the wind power into the power system will not reduce the system inertia if the control of a modern variable speed wind turbine is modified. These approaches shown that a short term active power support can be provided through the rotational energy stored in turbine blades. Nayeem Rahmat Ullah *et.al.* presented an approach to use rotational energy stored in turbine for maximum possible support of active power [4].

Mulane A. et.al.[5] discussed the inertial response of wind turbines employing induction machine based generators. The 5^{th} order model of field oriented doubly fed induction generator used in this work. The major findings of the work were on control of inertial effect by rotor current controller bandwidth. In [6-7] Nicholas W. Miller et.al. explains the dynamic of modeling of GE 1.5 Mw and 3.6 Mw WTGs. This paper provides the suggestion for dynamic modeling of the WTG for use in system impact studies. As the droop of a hydro turbine is much larger, the impact of WTGs on system frequency can be seen in hydro power plant and in the situation of generation shortage the drop is relatively higher in the case of hydro power plants [8].

Johan Morren et.al. presented a controller through which maximum power output is produced by maintaining the optimal speed of WTGs. The proposed controller in work [9] employed two signals i.e. frequency and rate of change of frequency. Authors demonstrated simulation with two thermal units and a six step variable WTG. Authors also reported that the rotational speed of wind turbine is reduced with frequency support. Since wind energy is discontinuous in nature and many designs of WTGs are available, the testing on each design and the behavior of machine in different contingencies is a matter of deep research. Moreover the above reported approaches established their designs on a single small perturbation. Janaka Ekanayake and Nick Jenkins [10] introduced a supplementary control loop in DFIG to achieve inertia with the evaluation of doubly fed and fixed speed induction generator.

In view of above discussion, the objectives of this paper are as follows:

1. To present a decisive study of wind farm participation on the system dynamics of two areas interconnected thermal power system.
2. To evaluate the impact of penetration levels on system dynamics through eigenvalue analysis.

3. To present the modeling of DFIG wind turbine as a frequency support. To establish the superiority of the proposed model through nonlinear simulation studies under different perturbation levels.
4. To optimize the integral gain parameters by using Grey Wolf Optimizer (GWO).

This paper presents the modeling and simulation results of two thermal area interconnected network with combination of DFIG based wind turbine. Eigen values are calculated at different wind penetration level to exhibit the impact of penetration on system dynamics. Further the non linear simulations are performed to validate the eigenvalue analysis. Frequency deviations of areas and tie line power exchanges show that DFIG supports the system frequency. A newly introduced optimization algorithm grey (GWO) wolf optimizer [11, 12] based on hunting behavior of grey wolves is employed to calculate the integral gains.

In the next section a brief description of modeling of the variable speed wind turbine system is presented. Section 3 evaluates the modified parameters with wind penetration. Section 4 describes the grey wolf optimization (GWO) technique. In Section 5, the results and simulations are presented at different wind penetration levels followed by conclusion.

2. WIND TURBINE MODELING

In this paper variable speed wind turbine based doubly fed induction generator (DFIG) is adopted. For variable speed operation, two back to back power electronic convertors are used which connects with the rotor to the grid. The model of multi-megawatt commercial variable speed wind turbine (GE 3.6 MW) is used here and is taken from [6, 7]. The block diagram of wind turbine model is shown in Fig. 1. Wind turbine converts the kinetic energy of the wind into the mechanical energy. The generated mechanical power is the complex function of three quantities i.e. wind speed, rotor speed and the pitch angle. The mechanical power is determined by

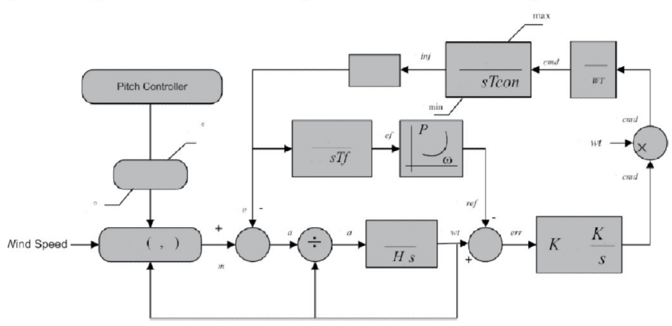

Fig. 1 Basic block diagram of variable speed wind turbine model [6,7]

$$P_m = \frac{\rho}{2} A_r v_w^3 C_p(\lambda, \theta) \tag{1}$$

Where P_m = mechanical power extracted from the wind, ρ = air density (kg/m^3, A_r = rotor swept area (m^2), v_w = wind speed (m/sec), C_p = power coefficient, which is function of (λ, θ). The power coefficient is defined as the fraction of power in a wind stream that can be extracted by a rotor and λ is the tip speed ratio and is termed as the ratio of rotor blade tip speed to the wind speed, θ is the blade pitch angle (degrees).

The mathematical representation of the Cp curves is obtained by:

$$\begin{aligned}C_p(\lambda,\theta) = {} & \alpha_{00}\theta^0\lambda^0 + \alpha_{01}\theta^0\lambda^1 + \alpha_{02}\theta^0\lambda^2 + \alpha_{03}\theta^0\lambda^3 + \\ & \alpha_{04}\theta^0\lambda^4 + \alpha_{10}\theta^1\lambda^0 + \alpha_{11}\theta^1\lambda^1 + \alpha_{12}\theta^1\lambda^2 + \alpha_{13}\theta^1\lambda^3 + \\ & \alpha_{14}\theta^1\lambda^4 + \alpha_{20}\theta^2\lambda^0 + \alpha_{21}\theta^2\lambda^1 + \alpha_{22}\theta^2\lambda^2 + \alpha_{23}\theta^2\lambda^3 + \\ & \alpha_{24}\theta^2\lambda^4 + \alpha_{30}\theta^3\lambda^0 + \alpha_{31}\theta^3\lambda^1 + \alpha_{32}\theta^3\lambda^2 + \alpha_{33}\theta^3\lambda^3 + \\ & \alpha_{34}\theta^3\lambda^4 + \alpha_{40}\theta^4\lambda^0 + \alpha_{41}\theta^4\lambda^1 + \alpha_{42}\theta^4\lambda^2 + \alpha_{43}\theta^4\lambda^3 + \\ & \alpha_{44}\theta^4\lambda^4\end{aligned} \tag{2}$$

Tip speed ratio, λ is calculated as:

$$\lambda = \omega_o R \frac{\omega_r}{v_w} \tag{3}$$

ω_r = speed of rotor (p.u.), v_w = wind speed (m/sec), ω_o = rotor base speed (rad/sec) and R = radius of rotor (m).

For the tracking of maximum power, reference speed is generated based on the measured electrical power.

Inertia computes the rotor speed. Per unit inertia constant, H is defined as kinetic energy stored in rotor at rated speed to the VA base [9]. Mathematically the inertia constant of GE turbine, H_{WT} is defined as:

$$H_{WT} = \frac{1}{2}\frac{J\omega_o^2}{3.6\times 10^6} \tag{4}$$

J = equivalent inertia of turbine-rotor (kg.m^2), ω_o = rotor base speed (rad/sec). The rotor inertia equation is given as:

$$J\omega_o \frac{d\omega_r}{dt} = T_m - T_e \tag{5}$$

Where T_m = mechanical torque and T_e = electromagnetic torque (N.m.).

Fig. 2 depicts the block diagram of two area interconnected power system. Both the area consists of non reheat thermal generating units along with DFIG-based wind turbine generators in each area. The parameters of the system are given in the Appendix. The dynamic behavior of the system is analyzed at different levels of wind penetrations. The proposed method is implemented using MATLAB 2013 and run on a Pentium IV CPU, 2.69 GHz, and 1.84 GB RAM computer [13]. Changes in system inertia and the speed regulation replace the linear model at different levels of wind penetration. To meet with the objective of AGC i.e. to regulate the system frequency and net power interchange in its scheduled range, the gains of the integral controller are to

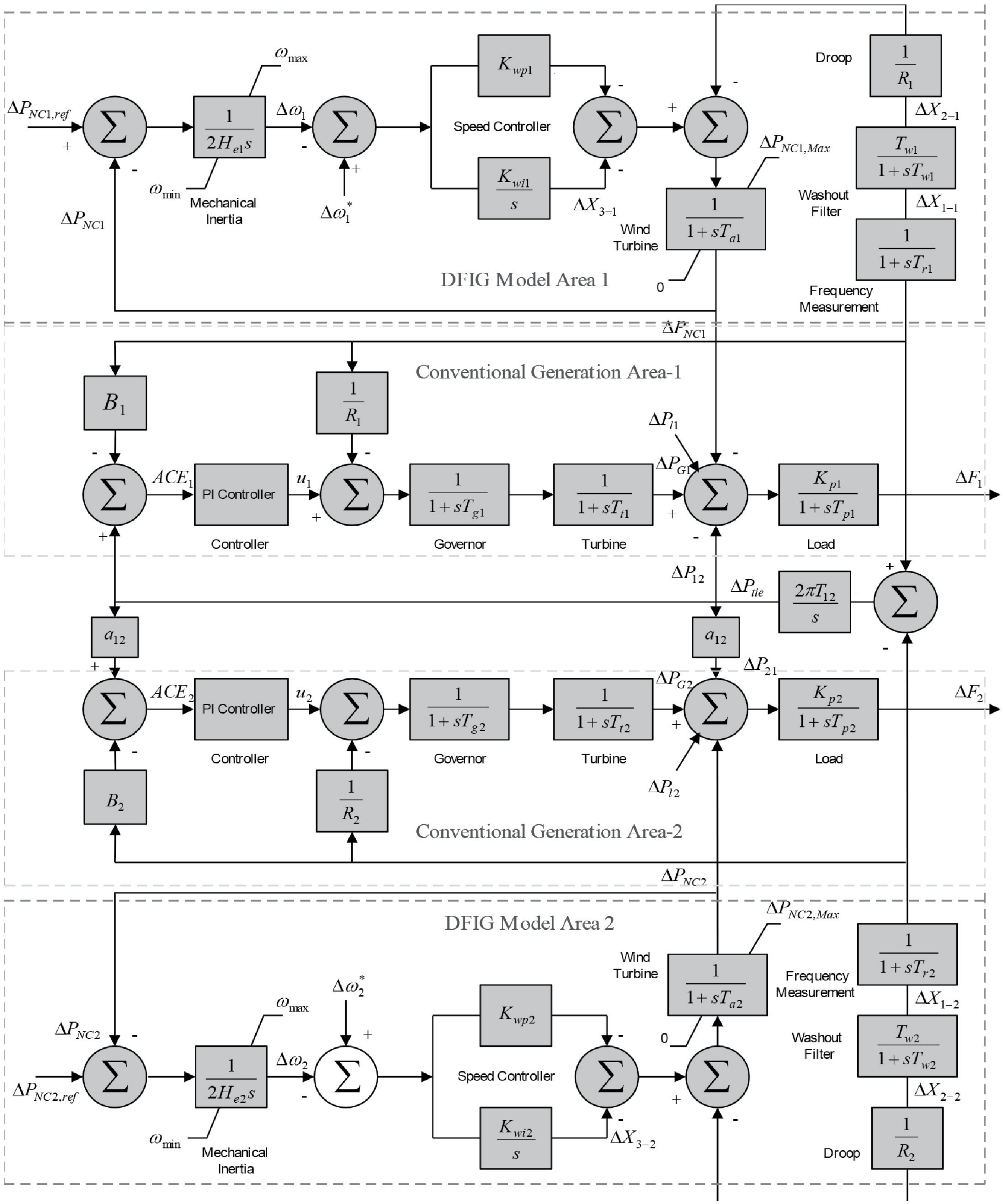

Fig. 2 Block diagram of two area interconnected thermal system with DFIG based wind turbines

be optimized. Integral of Time multiplied Absolute Error (ITAE) is used in this work as an objective function to minimize the error. The objective function is minimized by using Grey Wolf Optimizer. The objective function is defined as:

$$J = ITAE = \int_0^T (|\Delta f_1| + |\Delta f_2| + |\Delta P_{tie}|) \cdot t dt \quad (6)$$

The design problem can be formulated as:
Minimize J Subjected to

$$K_{I_{\min}} \le K_I \le K_{I_{\max}} \quad (7)$$

3. MODIFICATION OF THE PARAMETERS WITH THE WIND PENETRATION

The kinetic energy of the wind turbine is stored in the rotating mass of the blades. But variable speed wind turbine will not contribute kinetic energy to the inertia because it decouples the electrical and mechanical frequencies. Frequency support controller is used with the DFIG to release the stored kinetic energy in the blades of the turbine and emulates the system inertia. Maximum power is produced with the help of controller of variable speed wind turbine at its optimal speed. Hence, the system disturbance reduces with increased penetration of wind. Mathematically wind penetration can be defined as

$$Wind\ penetration\,(\%) = \frac{Total\ wind\ generation}{Total\ generation\ from\ sources} \times 100 \quad (8)$$

3.1 Change in regulation droop of the units.

For individual generators the regulation droop are same. With the increased penetration level the change in regulation droop is represented as [8]:

$$R_{Lp} = R/(1 - L_p) \quad (9)$$

3.2 Change in inertia constant without frequency support.

The number of generating units in the operation is reduced as the penetration level of the wind increases, which also reduces the system inertia. This will reduce the system frequency and raise the system disturbance without frequency support. Without frequency support the change in inertia constant is given by [8]:

$$H_{Lp} = H(1 - L_p) \quad (10)$$

3.3 Change in inertia constant with frequency support

The frequency support control of DFIG torque decouples the electrical and mechanical frequencies & provides the variable speed operation. As DFIG torque or speed not reflects any deviation in system speed similarly speed of convertor coupled generator does not depend on the grid frequency. Hence from the system point of view, DFIG has no inertia. The addition of frequency control signal with convertor signal enables the DFIG to modulate the inertia of the system [5, 9]

In the presence of wind penetration level, the modified inertia constant with frequency support is given by [4]:

$$H_{Lp} = H(1 - L_p) + H_e L_p \quad (11)$$

Where H_{Lp} is the modified inertia constant of wind penetration and H_e is the mechanical inertia of DFIG.

4. GREY WOLF OPTIMIZER

A recent population based swarm intelligence technique, called Grey Wolf Optimizer (GWO) inspired by the nature of grey wolf is discussed here. This technique was proposed by Mirjalili et.al. [11] in 2014. In GWO the leadership hierarchy and the hunting behavior of grey wolf is mimicked. GWO overcomes the possibility of local optimal solutions and has greater exploration and share information about the search space. Grey wolves are basically categorized into four groups namely alpha, beta, delta and omega for the simulation of leadership hierarchy. The three important steps of hunting, searching for prey, encircling the prey, and attacking towards prey are employed to carry out the optimization.

Alphas are the leaders of the pack. Alpha are decision makers regarding hunting, sleeping place and time to wake up etc and that decision will be followed by the pack. Hence, alpha wolf is also known as dominant wolf. Alpha is not essentially the strongest member in the pack but good in organization and discipline of the pack.

Beta comes in the second level on the hierarchy of grey wolves. Betas help alpha wolves in decision making and the activities of the pack. Betas are the best candidate to get the position of alpha in case of alpha wolves passes away or becomes very old. The beta supports alpha's command throughout the pack.

Omega wolves have the lowest ranking in the pack. They always have to surrender to all other dominant wolves. Omega is not a main member but everyone faces the fighting and problems in case of losing omega.

If a wolf is not coming in the above specified levels then he/she is delta wolves. Delta wolves have to submit alpha and beta but they dominate omega. Scouts, elders, hunters, sentinel and care takers belong to this group. According to Muro et.al. [12] below are the main stages of grey wolf hunting.

- Tracking, chasing and approaching the prey
- Pursuing, encircling and harassing the prey
- Attack towards the prey

In the mathematical modeling of social hierarchy of wolf, alpha (α) is considered as the fittest solution, beta (β) and delta (δ) are the second and the third best fittest solutions respectively in designing of GWO. The rest of the candidates solutions are considered as omega (ω). The hunting is guided by α, β and δ. The ω wolves follow α, β and δ wolves.

a. Encircling the prey

For the modeling of encircling the prey following equations are proposed

$$\vec{D} = \left| \vec{C}.\overrightarrow{X_P}(t) - \vec{X}(t) \right| \quad (12)$$

$$\vec{X}(t+1) = \overrightarrow{X_P}(t) - \vec{A}.\vec{D} \quad (13)$$

Where t represents current iteration, $\vec{A}$ and $\vec{C}$ are coefficient vectors, $\overrightarrow{X_P}$ is the position vector of the prey and $\vec{X}$ is the position vector of grey wolf.

The vectors $\vec{A}$ and $\vec{C}$ can be calculated as follows:

$$\vec{A} = 2\vec{a}.\vec{r_1} - \vec{a} \quad (14)$$

$$\vec{C} = 2.\vec{r_2} \quad (15)$$

The components of $\vec{a}$ are decreased linearly from 2 to 0 over the course of iterations and r_1, r_2 are random vectors in [0,1].

b. Hunting for the prey

During hunting, the first three best solutions (α,β,δ) obtained are saved and coerce the other search agents (including the omega) to update their positions according to the best search agent. The following are the proposed formula

$$\overrightarrow{D_\alpha} = \left|\overrightarrow{C_1}.\overrightarrow{X_\alpha} - \vec{X}\right|, \overrightarrow{D_\beta} = \left|\overrightarrow{C_2}.\overrightarrow{X_\beta} - \vec{X}\right|, \overrightarrow{D_\delta} = \left|\overrightarrow{C_3}.\overrightarrow{X_\delta} - \vec{X}\right| \quad (16)$$

$$\overrightarrow{X_1} = \overrightarrow{X_\alpha} - \overrightarrow{A_1}.(\overrightarrow{D_\alpha}), \overrightarrow{X_2} = \overrightarrow{X_\beta} - \overrightarrow{A_2}.(\overrightarrow{D_\beta}), \overrightarrow{X_3} = \overrightarrow{X_\delta} - \overrightarrow{A_3}.(\overrightarrow{D_\delta}) \quad (17)$$

$$\vec{X}(t+1) = \frac{X_1 + X_2 + X_3}{3} \quad (18)$$

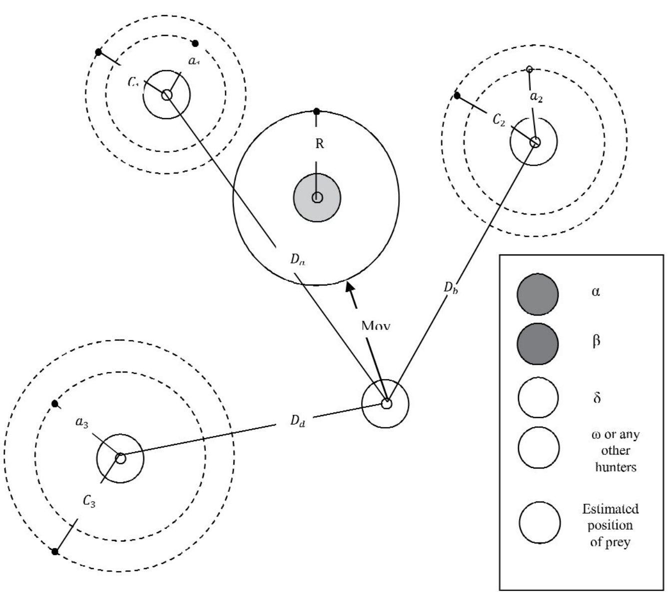

Fig. 3 Updating positions in GWO

Fig. 3 shows the updating position of search agent according to the alpha, beta and delta. It can be observed that alpha, beta and delta estimate the position of the prey and other wolves update their position stochastically around the prey and final position is randomly within the circle

c. Attacking towards the prey

When the prey stops moving, grey wolf finishes their hunt by attacking on it. Mathematically, as approaching towards the prey, the value of $\vec{a}$ decreases. Hence the fluctuation range of $\vec{A}$ is also decreased by $\vec{a}.\vec{A}$ is a random value in the interval [-a, a] where a is decreased from 2 to 0 over the course of iterations. When random values of $\vec{A}$ are in [-1, 1] the next position of a search agent can be in any position between its current position and the position of the prey. If |A|<1, grey wolves converge towards the prey and attacks on it.

d. Searching for the prey.

The searching of grey wolves depends on the position of the alpha, beta and delta. For searching, they diverge from each other. Mathematically $\vec{A}$ varies with random values greater than 1 or less than -1 to oblige the search agent to diverge from the prey. This brings out exploration and allows GWO algorithm to search globally. If |A|>1, grey wolves diverges from the prey to find the fitter prey.

5. SIMULATIONS AND RESULTS

Simulations have been made to examine the interaction of system between thermal plants and wind farms with different penetration levels of wind. The simulations are implemented on two area interconnected thermal system with DFIG based wind turbine using MATLAB/Simulink. The modeling of the system and simulation studies are performed over Intel ® core ™, i7, 2.9 GHz 4.00 GB RAM processor unit. To find the dynamic frequency responses and varying active power support from DFIG of the system with the implementation of AGC regulator these investigations have been carried out. Table 1 shows the system modes of the system with and without frequency support at different penetration levels of wind.

From the assessment of eigenvalues, it can be concluded that all the eigenvalue lie in the left half of s-plane, posses the negative real part and maintains the system stability. As the level of wind penetration increases, the negative real part of eigenvalues reduces and indicates the high oscillations in the system. It has also been observed that the eigenvalues have bigger negative part with the frequency support of DFIG as compared to without frequency support and improves the damping and overall dynamic stability of the system.

It is also observed from eigenvalue analysis that with 20% wind penetration level, significant amount of reduction in the real part of eigenvalues is found. With frequency support, a rational drift is observed in every penetration level. This provides a solid milieu for hypothesis that penetration of wind plants alone inculcates oscillatory instability. However, with proper design of pitch controller the droop support can be extracted from the kinetic energy stored in rotor blades.

Table 1: Eigenvalues at different level of penetration with and without frequency support

Wind Penetration	0%	10%	20%	30%	40%
With Frequency Support	-13.2826	-13.4109	-13.5737	-13.7824	-14.0588
	-13.2762	-13.4047	-13.5668	-13.7756	-14.0477
	-1.2480 ± 2.4444i	**-1.1927 ± 2.7478i**	**-1.1269 ± 3.0959i**	**-1.0329 ± 3.4976i**	**-0.9127 ± 3.9766i**
	-1.1394 ± 2.4230i	**-1.1016 ± 2.7364i**	**-1.0449 ± 3.0901i**	**-0.9646 ± 3.4979i**	**-0.8307 ± 3.9762i**
	-4.8509	-4.8509	-4.8509	-4.8509	-4.8508
	-0.3029 ± 0.1412i	**-0.2824 ± 0.1437i**	**-0.2646 ± 0.1440i**	**-0.2487 ± 0.1418i**	**-0.2500 ± 0.1420i**
	-0.1960 ± 0.1523i	**-0.1935 ± 0.1467i**	**-0.1882 ± 0.1372i**	**-0.1867 ± 0.1319i**	**-0.1830 ± 0.1227i**
	-0.0757 ± 0.0683i	**-0.0723 ± 0.0700i**	**-0.0663 ± 0.0726i**	**-0.0612 ± 0.0737i**	**-0.0560 ± 0.0736i**
	-0.0515 ± 0.0245i	**-0.0503 ± 0.0250i**	**-0.0485 ± 0.0257i**	**-0.0466 ± 0.0261i**	**-0.0457 ± 0.0266i**
	-0.0487	-0.0483	-0.0477	-0.0471	-0.0468
	-0.1342	-0.1342	-0.1339	-0.134	-0.1333
	-0.1483	-0.1474	-0.1464	-0.1453	-0.1452
Without Frequency Support	-13.2826	-13.442	-13.6529	-13.9389	-14.3408
	-13.2762	-13.4352	-13.6455	-13.9312	-14.3278
	-1.2480 ± 2.4444i	**-1.1825 ± 2.8172i**	**-1.0925 ± 3.2523i**	**-0.9644 ± 3.7748i**	**-0.7881 ± 4.4241i**
	-1.1394 ± 2.4230i	**-1.0886 ± 2.8060i**	**-1.0110 ± 3.2490i**	**-0.8962 ± 3.7781i**	**-0.7063 ± 4.4290i**
	-4.8509	-4.8509	-4.8509	-4.8508	-4.8508
	-0.3029 ± 0.1412i	**-0.2820 ± 0.1435i**	**-0.2640 ± 0.1432i**	**-0.2481 ± 0.1409i**	**-0.2493 ± 0.1410i**
	-0.1960 ± 0.1523i	**-0.1917 ± 0.1442i**	**-0.1883 ± 0.1366i**	**-0.1869 ± 0.1311i**	**-0.1832 ± 0.1220i**
	-0.0757 ± 0.0683i	**-0.0714 ± 0.0706i**	**-0.0662 ± 0.0726i**	**-0.0611 ± 0.0737i**	**-0.0559 ± 0.0736i**
	-0.0515 ± 0.0245i	**-0.0501 ± 0.0251i**	**-0.0485 ± 0.0257i**	**-0.0466 ± 0.0261i**	**-0.0457 ± 0.0266i**
	-0.0487	-0.0483	-0.0477	-0.0471	-0.0468
	-0.1342	-0.134	-0.1339	-0.1339	-0.1332
	-0.1483	-0.1474	-0.1464	-0.1453	-0.1452

The dynamic responses of two area interconnected thermal system with DFIG-based wind turbine are shown in Fig. 5-10. The analysis has been carried out for different levels of wind penetration (0, 10, 20, 30 and 40%) by taking speed regulation and inertia constant. The gains are optimized by using the PI controller with GWO. Integral Time multiplied Absolute Error (ITAE) is used as the objective function. For the superiority of the proposed approach, variable loading conditions have been taken. Fig. 4 shows the various loading conditions of the system

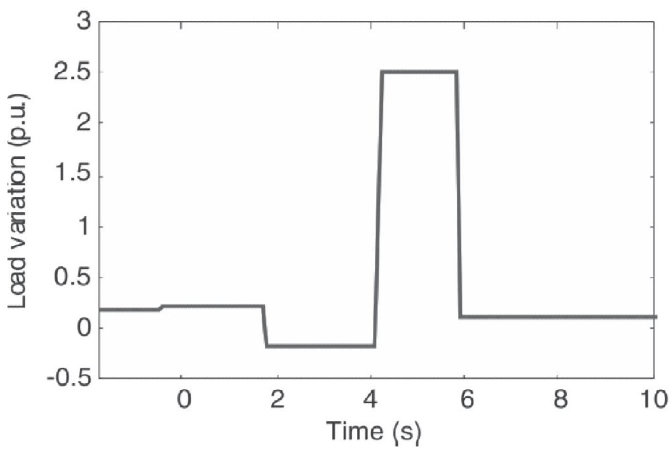

Fig. 4 Load variation in the system

Following are the two cases taken for the system investigation:
CASE A: With the frequency support of DFIG at different penetration levels of wind.
CASE B: Without frequency support of DFIG at different penetration levels of wind.

CASE A: The dynamic responses of deviation in frequency of area 1 and 2 with frequency support are shown in Fig. 5 and 6 respectively. It can be observed that with the increased penetration level of the wind, the inertia reduces and the system disturbance increases. Therefore, the system shows the highly oscillatory behavior and settling time. Hence it is concluded that larger penetration levels deteriorate the system dynamic performance with increased settling time and error.

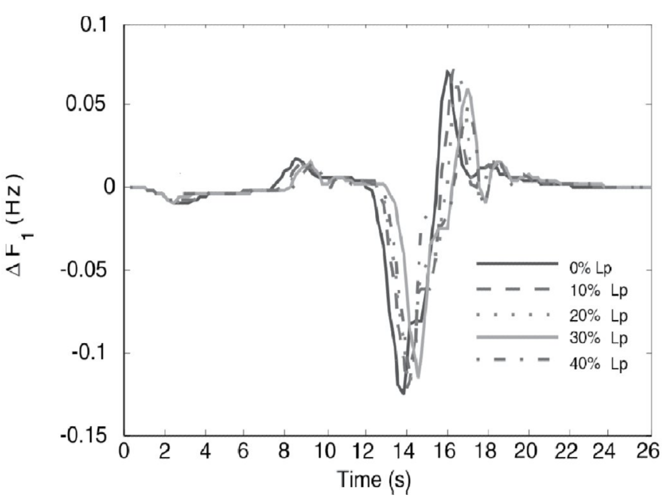

Fig. 5 Change in frequency of area 1 for different wind penetrations with frequency support

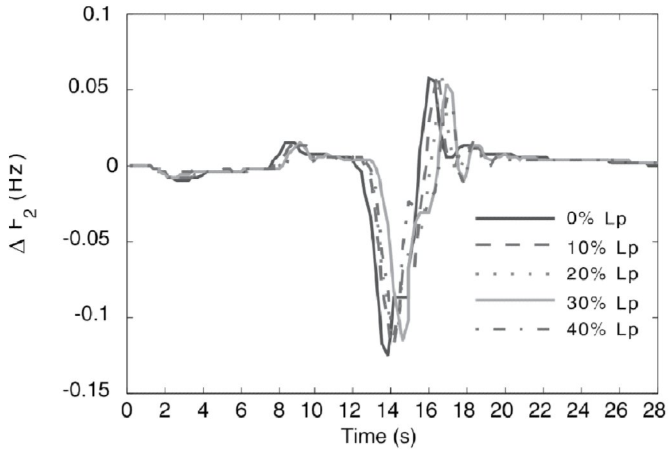

Fig. 6 Change in frequency of area 2 for different wind penetrations with frequency support

CASE B: Fig. 7 and 8 illustrates the dynamic responses of the system without frequency support of DFIG. It has been concluded that system retains its stability and quickly damped out the oscillations at less penetration level

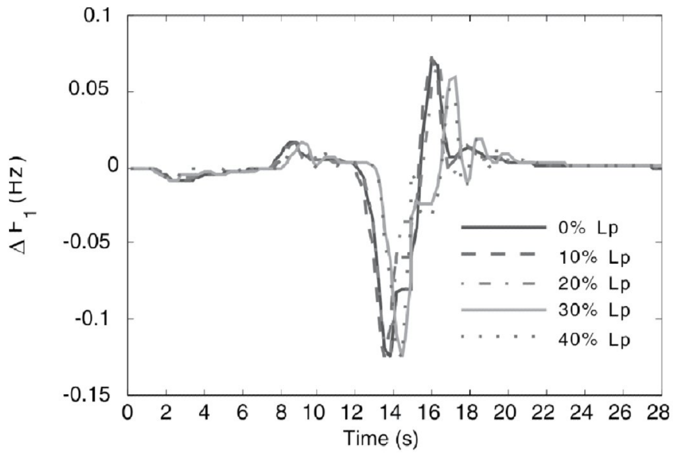

Fig. 7 Change in frequency of area 1 for different wind penetrations without frequency support

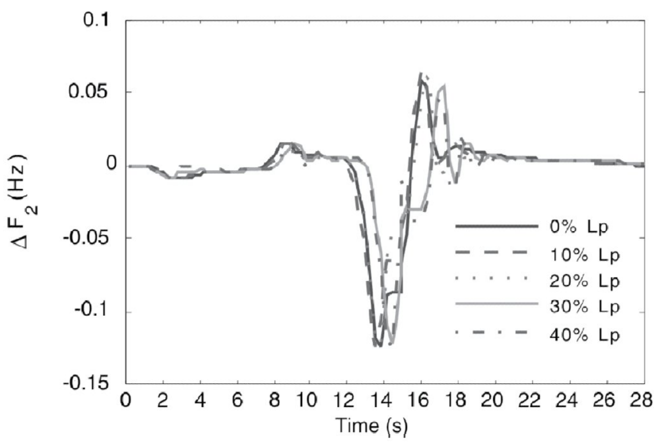

Fig. 8 Change in frequency of area 2 for different wind penetrations without frequency support

The dynamic responses of Δf_1 and Δf_2 at 40% of wind penetration are shown in Fig. 9 and 10. Figure shows the effect of wind penetration level when wind generators are participating with and without frequency support. The plots clearly illustrate that control the dip is smaller with the frequency support in wind generators as compared to without frequency support.

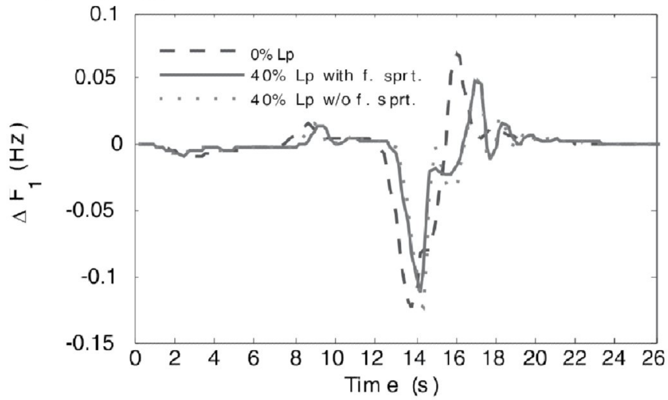

Fig. 9 Change in frequency of area 1 for 40% wind penetration with and without frequency support

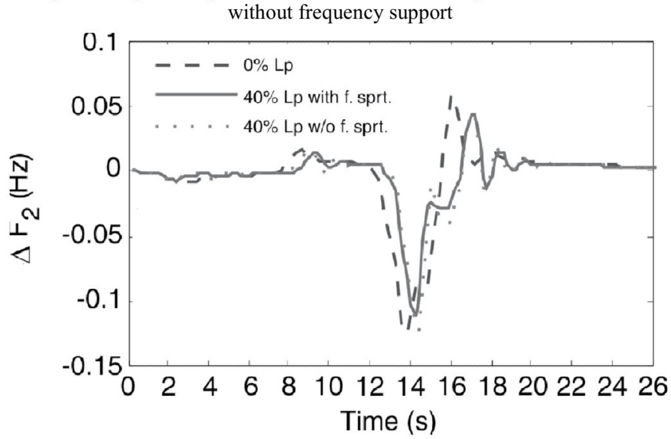

Fig. 10 Change in frequency of area 2 for 40% wind penetration with and without frequency support

6. CONCLUSION

Distributed generation sources have relieved the conventional grid from stressed conditions, wind power plants of higher penetration level not only shows the avenue for future smart grids but also provide a substantial growth in power generation. In this work the impact of wind penetration on frequency droop of two area interconnected thermal power system with DFIG based wind turbines is addressed. Following are the contributions of this manuscript:

a. GWO is used to optimize the integral gain parameters. The aim of this is to minimize the values of ITAE.

b. At different penetration levels the eigenvalue analysis is carried out for the efficacy of the system performance. The significant difference is found when different cases of frequency support are discussed and it is concluded that with small perturbation in the wind power plants support the frequency droop and offer an ease of control on system inertia.

c. It is also concluded that there is an appreciable reduction in the droops of frequency deviation when DFIG is participated with grid frequency

APPENDIX

1. Wind turbine parameters: $H_{e1} = H_{e2} = 3.5$ p.u. MW.sec, $K_{\omega p1} = K_{\omega p2} = 1$, $K_{\omega i1} = K_{\omega i2} = 0.1$, $T_{a1} = T_{a2} = 0.2$ sec, $T_{r1} = T_{r2} = 15$sec, $T_{w1} = T_{w2}$ = 6 sec.
2. Thermal unit parameters: $T_{12} = 0.545$ p.u.MW/Hz, $K_{p1} = K_{p2} = 120$ Hz/(p.u.MW), $T_{p1} = T_{p2} = 20$ sec, $T_{g1} = T_{g2} = 0.08$ sec, $T_{t1} = T_{t2} = 0.3$ sec, f= 60 Hz, $R_1 = R_2 =$ 2.4Hz/(p.u.MW), $B_1 = B_2 = 0.425$ p.u. MW/Hz-1, $a_{12} = -1$.

REFERENCES

[1] Kundur P., Power System Stability and Control. New York: McGraw-Hill; 1993

[2] Ackermann T., Ed., Wind Power in Power System. West Sussex, U.K: Willey; 2005

[3] Lalor G, Ritchie J, Rourke S, Flynn D, O'Malley M, "Dynamic frequency control with increasing wind generation," In: Proc. IEEE Power Eng. Soc. General meeting, vol. 2, 2004.

[4] Ullah Nayeem Rahmat, Thiringer Torbjorn, Karlsson Daniel, " Temporary primary frequency control support by variable speed wind turbines- potential and applications," IEEE Trans. Power System, vol. 23, no. 2, May 2008.

[5] Mulane A., O'Malley M, "The inertial response of induction machine based wind turbines," IEEE Trans. Power System, vol. 20, no. 3, pp. 1496-1503, Aug 2005.

[6] Miller NW, Sanchez-Gasca JJ, Price WW, Delmerico RW, "Dynamic modeling of GE 1.5 and 3.6MW wind turbine-generators for stability simulations," In: Proc. IEEE Power Eng. Soc. General meeting, pp. 1977-1983, Jul 2003

[7] Miller NW, Price WW, Sanchez-Gasca JJ, Dynamic modeling of GE 1.5 and 3.6MW wind turbine-generators. GE-Power System Energy Consulting; Tech. Rep. Version 3.0, Oct 2003.

[8] Bhatt P., Roy R., Ghoshal SP., "Dynamic participation of doubly fed induction generator in automatic generation control," Sci Direct Renew. Energy, pp. 1203-1213, 2011.

[9] Moren J, de Haan, SWH, Kling WL, Ferreira JA, "Wind turbines emulating inertia and supporting primary frequency control," IEEE Trans. Power System, vol. 21, no. 1, pp. 433-434, Feb 2006.

[10] Ekanayake J., Jenkins N., "Comparison of the response of doubley fed and fixed-speed induction generator wind turbines to change in network frequency," IEEE Trans. Energy Convers., vol. 19, no. 4, pp. 800-802, Dec 2004.

[11] Mirjalili S., Mirjalili S. M., Lewis A., "Grey Wolf Optimizer," Advances in Engineering Software, vol. 69, pp. 46-61, 2014.

[12] Muro C., Escobedo R., Spector L., Coppinger R., "Wolf-pack (Canis lupus) hunting strategies emerge from simple rules in computational simulations," Behavioural processes, vol. 88, pp. 192-197, 2011.

[13] MATLAB, Available:http://www.mathworks.com

◆ ◆ ◆